

1
2
3
4 **Macrophages Mediate the Anti-Tumor Effects of the Oncolytic Virus HSV1716 in**
5 **Mammary Tumors**
6
7

8 Amy Kwan¹, Natalie Winder¹, Emer Atkinson¹, Haider Al-Janabi¹, Richard J Allen¹, Russell
9 Hughes¹, Mohammed Moamin¹, Rikah Louie¹, Dhanajay Evans¹, Matthew Hutchinson¹,
10 Drew Capper¹, Katie Cox¹, Joshua Handley¹, Adam Wilshaw¹, Taewoo Kim¹, Simon J
11 Tazzyman¹, Sanjay Srivastava², Penelope Ottewell¹, Jayakumar Vadakekolathu^{3,4}, Graham
12 Pockley^{3,4}, Claire E Lewis^{1,5}, Janet E Brown^{1,5}, Sarah J Danson^{1,5}, Joe Conner⁶, Munitta
13 Muthana^{1,5}
14

15 ¹Department of Oncology and Metabolism, University of Sheffield Medical School, Sheffield,
16 S10 2RX, UK.

17 ²Department of Immunotherapeutics and Biotechnology and Center for Tumor Immunology
18 and Targeted Cancer Therapy, Texas Tech University Health Sciences Center, Abilene,
19 Texas, 79601, USA

20 ³John van Geest Cancer Research Centre, School of Science and Technology, Nottingham
21 Trent University, Nottingham, NG11 8NS, UK

22 ⁴Centre for Health and Understanding Disease (CHAUD), School of Science and
23 Technology, Nottingham Trent University, Nottingham, NG11 8NS, UK

24 ⁵Sheffield ECMC, Cancer Clinical Trials Centre, Weston Park Hospital, Sheffield, S10 2SJ,
25 UK

26 ⁶Virttu Biologics Ltd, BioCity Scotland, Bo'ness Rd, Newhouse, ML1 5UH, UK
27
28

29 **Running Title:** Oncolytic virus reprograms macrophages within the TME
30

31 **Key words:** macrophages, breast, oncolytic viruses, PCNA
32

33 **Corresponding Author:**

34 Dr Munitta Muthana
35 Department of Oncology and Metabolism
36 University of Sheffield Medical School
37 Beech Hill Road, Sheffield, S10 2RX, UK
38 Tel: + 44 114 2159057
39 Fax: + 44 114 2713314
40 Email: m.muthana@sheffield.ac.uk
41

42 **Conflict of interest disclosure statement:** J. Conner is an employee of Virttu
43 Biologics/Sorrento Therapeutics who own HSV1716.
44
45
46
47
48
49

50 Abstract 247

51 Word count: 5735. Reference count: 50. Figure count: 7. Supplementary Figures and
52 Tables: 11
53
54
55

1
2
3
4
5
6
7
8
9
10
11
12
13
14
15
16
17
18
19
20
21
22
23
24
25
26
27
28
29
30
31
32
33

Financial information:

- Cancer Research UK (CRUK grant reference: C25574/A24321)
- Sheffield Teaching Hospitals (grant reference: 12053)
- Team Verrico (grant reference: MS/149394)
- European Union's Horizon 2020 (Marie Skłodowska-Curie grant (872860-PRISAR2))

1 **Abstract**

2 Oncolytic viruses (OV) have been shown to activate the anti-tumor functions of specific
3 immune cells like T cells. Here, we show OV can also reprogram TAMs to a less
4 immunosuppressive phenotype. Syngeneic, immunocompetent mouse models of primary
5 breast cancer were established using PyMT-TS1, 4T1 and E0771 cell lines and a metastatic
6 model of breast cancer was established using the 4T1 cell line. Tumor growth and overall
7 survival was assessed following intravenous administration of the OV, HSV1716 (a modified
8 herpes simplex virus). Infiltration and function of various immune effector cells was assessed
9 by NanoString, flow cytometry of dispersed tumors and immunofluorescence analysis of
10 tumor sections. HSV1716 administration led to marked tumor shrinkage in primary mammary
11 tumors and a decrease in metastases. This was associated with a significant increase in the
12 recruitment/activation of cytotoxic T cells, a reduction in the presence of regulatory T cells
13 and the reprogramming of TAMs towards a pro-inflammatory, less immunosuppressive
14 phenotype. These findings were supported by *in vitro* data demonstrating that human
15 monocyte-derived macrophages (MDMs) host HSV1716 replication, and that this led to
16 immunogenic macrophage lysis. These events were dependent on macrophage expression
17 of proliferating cell nuclear antigen (PCNA). Finally, the anti-tumor effect of OV was
18 markedly diminished when TAMs were depleted using clodronate liposomes. Together, our
19 results show that TAMs play an essential role in support of the tumoricidal effect of the OV,
20 HSV1716 – they both host viral replication via a novel, PCNA-dependent mechanism and
21 are reprogramed to express a less immunosuppressive phenotype.

22

1 **Introduction**

2 Although modulating the immune system to target cancer has been a successful treatment
3 for some solid malignancies, various forms of breast cancer are immunogenically cold [1] in
4 that they exhibit a decreased mutational load and neoantigen expression. This leads to a
5 lower infiltration by activated cytotoxic T cells and is often accompanied by a highly
6 immunosuppressive tumor microenvironment (TME) resulting in an intrinsic resistance to
7 immunotherapies. The TME consists of cancer cells, tumor vasculature, fibroblasts,
8 mesenchymal stem cells, adipocytes, extracellular matrix and immune system elements
9 such as lymphocytes and tumor-associated macrophages (TAMs). TAMs are a key
10 component of the TME that contribute to immune evasion, suppress lymphocyte activity and
11 support tumor growth [2, 3]. In particular, the accumulation of perivascular M2-skewed
12 TAMs on the abluminal surface of tumor blood vessels has been shown to drive tumor
13 relapse following radiotherapy [4] and chemotherapy [5], perhaps contributing to the
14 eventual resistance of these standards of care [5, 6]. A shift in the composition of the TME,
15 together, with a burst in the release of tumor antigens, may turn a 'cold' tumor into a 'hot'
16 one and therefore allow the host's immune system to recognise and halt tumor growth and
17 metastasis [7].

18

19 Oncolytic viruses (OV) are a promising class of anti-cancer therapeutics which replicate in
20 malignant cells and stimulate anti-tumor responses by initiating immunogenic cancer cell
21 death (ICD), activating T cells and inducing protective anti-tumor immunity. Preclinical and
22 early phase clinical studies, in a number of solid tumor types including breast cancer have
23 shown OV to have therapeutic efficacy with minimal toxicity [8-10].

24

25 HSV1716 is an OV derived from the Herpes Simplex Virus HSV-1 strain 17. It possesses a
26 deletion in the RL1 genes encoding ICP34.5. Mutants lacking ICP34.5 are selectively
27 replication competent in cancer cells. The subsequent lysis of these cells induces anti-tumor
28 immune responses both directly, through cell lysis, and indirectly, via the induction of

1 immunogenic cell death and stimulation of adaptive immunity [11]. As HSV1716 maintains
2 expression of thymidine kinase, its toxicity is reversible by administering the anti-viral
3 acyclovir, thereby providing a "therapeutic safety net" to clinical toxicity. Phase I/II trials in
4 over 100 paediatric and adult patients with solid malignancies have demonstrated minimal
5 systemic toxicity when HSV1716 is administered intratumorally (IT), intravenously (IV) or
6 loco-regionally [12, 13].

7

8 Here, we show that HSV1716 effectively reduces primary and metastatic mouse breast
9 tumors *in vivo*, in part, by replicating within and reprogramming macrophages in the TME.

10

11 **Materials and Methods**

12 **Cell lines and culture**

13 Murine PyMT-TS1 [14] (a kind gift from Prof Johanna Joyce, Memorial Sloan Kettering
14 Cancer Center (MSKCC), USA), E0771 (obtained from Dr Jessalyin Ubellacker (Harvard
15 University, USA) and LUC-4T1-BR [15] (obtained from Prof Sanjay Srivastava, University of
16 Texas, USA) mammary cancer cells were used *in vivo*. Human MCF-7, MDA-MB-231,
17 MCF10DCIS and SKBR3 cells, murine 4T1, EO771 and PyMT-TS1 cells and African Green
18 Monkey Vero cell lines were used *in vitro*. Unless specified, all cell lines were purchased
19 from the ATCC between 2015-2018 and used within 30 passages. Murine E0771 and human
20 MDA-MB-231 cells were maintained in RPMI supplemented with 10% v/v fetal bovine serum
21 (FBS) and 1% L-glutamine. Murine Luc-4T1-BR cells (4T1 cells transfected to express
22 luciferase) were maintained in Dulbecco's Modified Eagle's Medium (DMEM) supplemented
23 with 10% v/v FBS. All cells were used within 20 passages and were cultured at 37°C in 5%
24 v/v CO₂. The identities of all cell lines were regularly confirmed using microsatellite analysis
25 and were tested to be mycoplasma free. All culture reagents were purchased from Lonzo
26 BioWhittaker Ltd.

27

28

1 **Preparation of monocyte-derived macrophages (MDMs)**

2 Human monocytes were isolated from mononuclear cells derived from human buffy coats
3 obtained from the NHS Blood and Transplant Unit, Sheffield, as previously described [16].
4 Briefly, the peripheral blood mononuclear cell (PBMC) layer was collected following
5 centrifugation over Ficoll (Sigma-Aldrich, UK) and seeded overnight in Iscove's Modified
6 Dulbecco's Medium (IMDM, Sigma-Aldrich, UK) and 2% v/v human AB serum (Sigma
7 Aldrich, UK). Non-adherent cells were removed, and macrophages allowed to fully
8 differentiate.

9

10 **Virus production and handling**

11 HSV1716 (unlabelled) and HSV1716-GFP (in which GFP is driven by a CMV promoter) were
12 obtained from Virttu Biologics (Glasgow, UK) in stocks of 1×10^8 Particle Forming Units (PFU)
13 in compound sodium lactate (Hartmann's solution) with 10% v/v glycerol. All vials were
14 stored at -80°C and freshly thawed on ice immediately before each experiment.

15

16 **HSV1716 infection of MDMs *in vitro***

17 MDMs were washed in phosphate buffered saline (PBS), suspended in 500 μL serum-free
18 RPMI medium and then incubated with HSV1716 virus (MOI 5) for 2 hours at 37°C in 5% v/v
19 CO_2 . Non-infected virus was washed off and cells were analysed 24-72 hours post infection.
20 For plaque assays supernatants were removed at each time point and added to Vero cells
21 as described below.

22

23 **Mixed lymphocyte reaction (MLR)**

24 A Mixed Lymphocyte Reaction (MLR) was used to identify leukocyte activation and
25 proliferation in an autologous reaction. MDMs were obtained from human buffy coats and
26 cultured as above. Lymphocytes, from the same donor, were frozen down in 90% v/v
27 FBS+10% v/v dimethyl sulfoxide (DMSO) until needed. Once mature, MDMs alone or MDMs
28 infected with HSV1716 for 4 hours were co-incubated with lymphocytes at a ratio of 1:6, as

1 described previously [17]. MDA-MB-231 cells were also added, if needed, at a 1:1 ratio with
2 MDMs. Lymphocytes were co-cultured with macrophages for 24 hours before analysis by
3 flow cytometry.

4

5 **Flow cytometric analysis**

6 MDMs (24 hours after infection) and dissociated mammary tumors were stained with
7 fluorescent antibodies (Supplementary Table S1) [5]. All antibody incubations were
8 performed for 1 hour at 4°C and the samples were analysed using an BD™ LSR II flow
9 cytometer (BD Biosciences, Franklin Lakes, NJ, USA) and data analyzed processed using
10 FlowJo™ Flow Cytometric Data Analysis Software (BD Biosciences). The mouse immune
11 cell populations analysed included: neutrophils (CD45⁺CD11b⁺Ly6G⁺), monocytes
12 (CD45⁺CD11b⁺Ly6G^{neg}Ly6C⁺F4/80^{Lo}), macrophages (CD45⁺CD11b⁺Ly6G^{neg}Ly6C^{Lo}F4/80^{Hi}),
13 T_{Helper} (CD45⁺CD3⁺CD4⁺) and cytotoxic T-cells (CD45⁺CD3⁺CD8⁺). The membrane
14 impermeant, fixable, amine reactive dye Zombie UV™ Fixable (BioLegend Inc., San Diego,
15 CA, USA) was used to discriminate between live and dead cells. All data are presented as
16 the proportion of viable leukocytes.

17

18 **Real-Time PCR (qPCR)**

19 Total mRNA was extracted from cultured MDMs or murine tissues using the RNeasy™ Mini
20 Kit (Qiagen). A list of primer sequences is given in Supplementary Table S2. The Ct values
21 generated from these samples were normalized to a housekeeping gene. Relative gene
22 expression to untreated macrophages was estimated via normalisation of the gene of
23 interest to the housekeeping gene followed by the comparative Ct ($2^{-\Delta\Delta Ct}$) method.

24

25 **Western blot analysis**

26 Protein detection by SDS-PAGE was carried out on MDMs [18]. Protein samples were
27 denatured at 70°C and loaded onto a gel with Laemmli sample buffer. The gel was
28 transferred onto a nitrocellulose membrane (Invitrogen) using an iBlot gel transfer device.

1 The membrane was blocked in 5% v/v milk for an hour and incubated, at room temperature,
2 with primary antibodies for 90 minutes and secondary antibodies for an hour. Membranes
3 were probed with enhanced chemiluminescence (ECL) (BIO-RAD) and visualised using a
4 Chemidoc 2011 (BIO-RAD).

5

6 **HSV1716-induced cell lysis**

7 To assess cell lysis induced by HSV1716, various cell lines were seeded at 1×10^5 cells/well
8 in a 24 well plate and infected with HSV1716 at MOI 5 (unless otherwise stated). At 24 and
9 48 hours, cells were stained with $2 \mu\text{g/ml}$ propidium iodide (PI). Cell numbers and PI positivity
10 were analysed on the BD™ LRSII flow cytometer (Thermo Fischer Scientific). FlowJo™
11 software was used to analyse cell death based on a change in fluorescence against FL3-H
12 for PI and FL1-H for GFP expression.

13

14 **Viral replication**

15 qPCR: RNA was isolated from infected MDMs using the RNeasy Mini Kit (Qiagen) followed
16 by cDNA synthesis using SuperScript™ III Reverse Transcriptase (Life Technologies,
17 Paisley, UK). cDNA was analyzed using viral replication genes *ICP0*, *ICP8* and gB with
18 *GAPDH* as the housekeeping gene using SYBR™ Green (Primer Design, Chandler's Ford,
19 UK) (see Supplementary Table S2).

20

21 *In vivo* viral detection: Immunohistochemistry was carried out on fixed tissue sections
22 stained using a polyclonal sheep HSV antibody at a dilution of 1:500 (kind gift from Virttu
23 Biologics) for 1 hour. Staining was then visualized using a sheep VECTASTAIN™ ABC HRP
24 (Horseradish Peroxidase) Kit (Vector Laboratories, Peterborough, UK). Slides were counter
25 stained, mounted and sections scanned using Hamamatsu NanoZoomer XR (Hamamatsu,
26 Hertfordshire, UK).

27

1 Plaque assays: These were performed as described previously by Baer and Kehn-Hall [19].
2 Briefly, confluent monolayers of Vero cells were inoculated with serial dilutions of
3 supernatants derived from infected macrophages as described above. After 2 hours,
4 supernatants were removed and monolayers were overlaid with 4% w/v agarose:culture
5 medium (1:10) which was allowed to solidify for 15 minutes at room temperature before
6 incubation in a humidified incubator for 72 hours at 37°C. Paraformaldehyde (4% w/v) was
7 applied to agarose plugs for 1 hour to fix the cell monolayers before their removal. Cells
8 were washed with PBS, stained with 1ml crystal violet for 5 minutes and rinsed with tap
9 water. Once dried, plaques were counted per well and viral titre determined.

10

11 **Analysis of MDM death**

12 To understand how HSV1716 mediated the oncolysis of MDMs *in vitro*, the expression of a
13 panel of cell death markers was determined using qPCR. cDNA was analyzed using a pre-
14 designed apoptosis and survival array (tier 1) (BIO-RAD, Hertfordshire, UK) and then
15 validated by qPCR using a panel of apoptotic genes (*FASL* and *BCL2*), autophagy genes
16 (*ATG5* and *LC3B*) and ICD genes (*HMGB1* and *CalR*), with *GAPDH* as the housekeeping
17 gene (see Supplementary Table S2). Analysis using a HMGB1 ELISA Kit II (Shino-Test,
18 Kanagawa, Japan) and an ENLITEN ATP assay (Promega, Madison, WI, USA) confirmed
19 the presence of immunogenic cell death (ICD).

20

21 **Knockdown of PCNA expression in MDMs**

22 MDMs were transfected with PCNA or nonspecific siRNAs (Accell Human PCNA siRNA
23 SMARTpool, 10nmol, Thermo Scientific/Dharmacon). For this, MDMs were aliquoted into a
24 6-well plate (0.5×10^5 macrophages/well) and incubated with 1.5ml of Accell delivery
25 medium containing 1 μ M siRNA, after which they were incubated at 37°C for 72 hours.
26 Protein or mRNA knockdowns were confirmed by Western blot and qPCR and viability
27 determined using the MTS CellTiter 96™ AQueous One Solution Cell Proliferation Assay
28 (Promega).

1 ***In vivo studies***

2 Animal procedures were carried out in accordance with the UK Animals (Scientific
3 Procedures) Act 1986 with approval from the UK Home Office approval (PPL70/8670), the
4 ARRIVE (Animal Research: Reporting of In Vivo Experiments) guidelines and the University
5 of Sheffield Animal Welfare Ethical Review Body (AWERB). All female mice were obtained
6 from Charles River Laboratory at 6-8 weeks and acclimatised in the Biological Services
7 Laboratory for 7 days prior to experimentation. Animals were anaesthetised using 3-4%
8 isoflurane in 70:30% N₂O:O₂.

9

10 *Orthotopic mammary tumor model:* Mammary cancer cells (1x10⁶ PyMT TS1 cells in 50µl of
11 1:1 Matrigel™), were implanted into the 4th mammary fat pads of 6-7 week old syngeneic
12 FVB mice (n=10/group). E0771 and 4T1 cells were implanted via intraductal injection to the
13 mammary fat pads of syngeneic C57BL/6 and BALB/c mice respectively. Mammary tumor
14 growth was assessed by digital calliper measurement every 2-3 days and when tumors
15 reached 150mm³, mice were randomly divided into groups and received a single 100µl
16 injection of PBS or HSV1716 (1x10⁶ PFU) intravenously via tail vein injection. Of note, a
17 similar treatment schedule, was performed to compare intravenous (IV) and intratumoral (IT)
18 injections in the PyMT TS1 model. Of note, mice in the PBS groups became unwell at day 9
19 and therefore some mice, in both groups, were culled early for post-mortem comparison of
20 tissues. Excised tissues (tumors, brain, liver, lungs, kidney and spleen) were embedded in
21 OCT freezing media or paraffin wax for immunocytochemical and histological labeling
22 studies. Tumors were dispersed by enzymatic digestion after first dicing into approximately
23 1mm³ pieces. These pieces were incubated for 40 minutes at 37°C in serum-free IMDM
24 (VWR International, PA, USA) supplemented with 2mg/mL dispase, 0.2mg/mL collagenase
25 IV (Sigma Aldrich, St. Louis, MO, USA) and 100U/mL DNase (Merck Millipore, Burlington,
26 MA, USA). Dispersed tumors were passed through 70µm nylon filters (Becton Dickinson,
27 Franklin Lakes, NJ, USA) and maintained on ice in PBS or cryo-preserved in 90% v/v FBS
28 and 10% v/v DMSO for flow cytometric analysis.

1 *Experimental metastasis model:* To model the metastatic seeding seen in breast cancer
2 patients, we used a metastatic 4T1 cell line which metastasises to brain, lung, liver and
3 bones when administered via intracardiac route[15]. For this model, 1×10^5 LUC-4T1-BR cells
4 were filtered and injected into the left ventricle of 6-7-week-old female BALB/c mice. Tumors
5 were allowed to grow for 5 days following which animals were randomly allocated (n=6 per
6 group) and received either PBS, 1 dose of HSV1716 (1×10^7) or 3 doses of HSV1716 (1×10^7
7 given on day 1, 3 and 5). Animals were imaged 2-3 times a week using a luminescence *in*
8 *vivo* imaging system (IVIS Lumina II imaging, Caliper Life Sciences) following intra-
9 peritoneal injection of luciferin (150mg/kg). Mice were sacrificed if they reached a humane
10 end point (weight loss over 20%, signs of distress (e.g. breathlessness or pain) or the
11 experimental end point of 50 days following tumour inoculation. Weight loss was the most
12 common cause of premature sacrifice.

13

14 *Macrophage depletion model:* Macrophages were depleted using a single dose of clodronate
15 liposomes (CL) (Liposoma B.V.) 48 hours prior to viral administration in the primary
16 mammary model. When mammary tumors reached 150mm^3 , animals were divided into 4
17 groups, n=5/group. Control groups received either 1 dose of PBS (100 μ l) or 1 dose of
18 clodronate liposomes (100 μ l). Treatment groups received an intravenous injection of
19 HSV1716 (1 dose, 1×10^6 PFU) or intravenous injection of CL followed by intravenous
20 HSV1716 (1 dose, 1×10^6 PFU). Animals were monitored and primary tumors measured
21 every 2-3 days using callipers. All animals were culled as soon as one animal had a tumor of
22 800mm^3 .

23

24 **Tissue Analysis**

25 Frozen tumor sections were blocked with 1% w/v BSA and 5% v/v goat serum for 30 minutes
26 and incubated, at room temperature, with the relevant primary antibodies (Supplementary
27 Table S1), for an hour. Alexa Fluor™-conjugated anti-rabbit or anti-rat secondary antibodies
28 (as appropriate) were used to detect primary antibody binding. Nuclei in all tumor sections

1 were counterstained with DAPI. Slides were visualised using a Nikon DualCam system
2 microscope, a Nikon A1 Confocal Laser Microscope and an EVOS™ Cell Imaging System
3 (ThermoFisher). Formalin-fixed, paraffin-embedded tissues were rehydrated, peroxidase
4 blocked, antigen retrieved, serum blocked, and then incubated with primary antibodies for 1-
5 2 hours. Primary antibodies were detected with ABC or Polymer detection kits followed by
6 chromogen staining with 3'-Diaminobenzidine (DAB). Following Haematoxylin and Eosin
7 staining, slides were visualized using the Hamamatsu NanoZoomer XR scanner
8 (Hamamatsu, Hertfordshire, UK) and staining in 5 randomly selected fields of view per tumor
9 quantified using ImageScope (Leica Biosystems).

10 **NanoString nCounter™ gene expression analysis**

11 Amplification-free gene expression profiling of tumor tissue using a NanoString nCounter™
12 FLEX platform and the murine PanCancer Immune Profiling Panel, which consist of 750
13 immune related genes and 20 housekeeping genes (NanoString Technologies Inc) was
14 undertaken in the John van Geest Cancer Research Centre (Nottingham Trent University).
15 Total mRNA was extracted from cultured MDMs or murine tissues using the RNeasy™ Mini
16 Kit (Qiagen) and quality controlled using a NanoDrop™ 8000 Spectrophotometer. For gene
17 expression profiling, 150ng of total RNA from each sample was used for NanoString probe
18 hybridisation which was undertaken overnight (20 hours) at 65°C in a PCR machine with
19 heated lid (each reaction mixture contains 5µl of RNA solution (150ng), 8µl of reporter probe
20 and 2µl of capture probe). After overnight hybridization, excess probes were removed using
21 the NanoString nCounter™ Prep Station and magnetic beads, hybridized mRNA/probe were
22 immobilised on a streptavidin-coated cartridge. The processed cartridge was subsequently
23 scanned, and raw data generated at high-resolution (555 fields of view, fov) using a
24 NanoString nCounter™ digital analyser platform and processed using nSolver™ Data
25 Analysis Software (V.4.0). Imaging quality control (QC), mRNA positive control QC and
26 normalisation QC were checked, and all the samples were with the quality parameters of
27 NanoString gene expression assays. Differential expression, pathway and cell type scoring

1 was performed using the nSolver™ Advanced Analysis Module v.2.0.115. Data
2 normalization was performed using the geNorm algorithm for the selection of the best
3 housekeeping genes. Genes which showed ≥ 2 , fold change in their expression with a BY
4 (Benjamini-Yekutieli procedure) P value ≤ 0.05 were considered significantly different
5 between the groups.

6

7 **Apoptosis and pro-survival array**

8 The Apoptosis and Pro-Survival Tier 1 array (BIO-RAD) was used to assess cell death. For
9 this, cDNA was synthesised from control or infected MDMs using the Precision nanoScript2
10 Reverse Transcription Kit (PrimerDesign). cDNA was plated into the 386 well qPCR plate
11 and processed using an Applied Biosystems 7900 Real-Time PCR System.

12

13 **Statistics**

14 All statistical analyses were performed using GraphPad Prism 8 and the tests are described
15 in the Figure legends. Data are means \pm SEM (as indicated) and P values of < 0.05 were
16 considered statistically significant.

17

18 **Results**

19 **HSV1716 has anti-tumor activity in breast cancer models**

20 The susceptibility of breast cancer cells to HSV1716 infection (Supplementary Fig. S1A) and
21 virus-mediated death (Supplementary Fig. S1B) was demonstrated *in vitro* using a panel of
22 human and murine breast cancer cells lines (MCF7, MDA-MB-231, SKBR3,
23 MCF10DCIS.com, 4T1, EO771, and PyMT-TS1).

24

25 The cytotoxic potential of HSV1716 was then assessed in three *in vivo* models of primary
26 breast cancer. First, we investigated the best route of HSV1716 delivery in the PyMT-TS1
27 model. For this, animals were randomly assigned into one of 3 treatment groups; control
28 (PBS), intratumoral (IT) HSV1716 and intravenous (IV) HSV1716, with a reduction in primary

1 mammary tumor growth being observed in both the IT and IV groups (Supplementary Fig.
2 S2A). IT and IV administration of HSV1716 also reduced pulmonary metastasis and
3 increased tumor necrosis (Supplementary Fig. S2B and S2C). Given the positive response
4 to IV HSV1716, and that the IV route is currently the preferred modality to deliver breast
5 cancer chemotherapies, the remainder of the study focused on IV delivery of HSV1716.

6
7 In three models of primary breast cancer (PyMT-TS1, E0771 and 4T1) we demonstrated IV
8 HSV1716 to significantly slow the growth of orthotopically implanted tumors (Figure 1A). The
9 number of subsequent spontaneous lung metastases in these animals was also significantly
10 reduced in the IV treated groups (Figure 1B). Furthermore, we observed that early
11 introduction of HSV1716 prevented the formation of breast cancer metastases and thereby
12 increased overall survival in the metastatic 4T1 model. In this model, luciferase labelled 4T1
13 cells were injected into the left ventricle of the heart. Five days later, mice were treated with
14 PBS, HSV1716 (1 dose) or HSV1716 (3 doses). Doses were repeated every 48 hours
15 (Figure 2A). Tumor growth and spread were monitored using bioluminescent *in vivo* imaging
16 2-3 times weekly (Figure 2B). A survival advantage was seen in the HSV1716 treated
17 groups over the PBS control, and a significant number of animals showed no sign of disease
18 by day 50 (Figure 2C). As shown, this was more marked with repeated doses of the virus, in
19 which instance, all mice survived to the experimental endpoint (50 days) compared to an
20 average survival of 31 days for one dose and 24.5 days for PBS mice ($p=0.0002$, CI 15.49-
21 35.18). This may be because the immunomodulatory effects of the virus takes time to
22 develop and repeated dosing allows for this to occur, or that repeat dosing does not allow
23 circulating tumor cells or micro-metastases to develop. The presence of brain, liver and lung
24 metastasis was assessed and a significant reduction in the number of lung metastases in the
25 groups treated with HSV1716 observed, with a trend to less metastases in the brain and liver
26 (Figure 2D). Together, these exciting results support the possible use of HSV1716 to treat
27 breast cancer.

28

1 **HSV1716 stimulates leukocyte infiltration into tumors**

2 The influence of HSV1716 treatment on the immune content of the TME, including immune
3 infiltrates was examined using the NanoString nCounter™ Mouse PanCancer Immune
4 Profiling Panel. This large targeted gene panel comprised of specific gene sets to
5 understand different immune cell types and their functions in the TME. As shown in Figure
6 3A treatment with HSV1716 induced the differential regulation of 282 genes (where $p=0.05$).
7 The top 20 genes and their biological functions are highlighted in Supplementary Table 3,
8 and these include genes involved in innate and adaptive immune responses (e.g. CD55, IL-
9 21, TXk, Thbs1), immune cell function (CD22, CD37, Blnk, Sell, CD247, IL7R, Dpp4, Btla,
10 CD247, Thbs1) and the TNF pathway (TNFRsf13b, Ltb). Supplementary Fig. 3A shows
11 genes related to upregulated pathways including innate and adaptive immunity,
12 inflammation, cytokines and receptors, apoptosis and cell type scores (dendritic cell, natural
13 killer, macrophages and T cells) that were significantly upregulated following intravenous
14 HSV1716 (Supplementary Fig. 3B).

15 To confirm the presence of these immune cells in the TME, flow cytometric analysis of
16 dispersed PyMT primary tumors demonstrated a significant increase in CD11b⁺Ly6C⁺
17 monocytes, CD11b⁺, LY6G⁺ neutrophils, CD3⁺ T cells, and CD8⁺ cytotoxic T cells following
18 HSV1716 treatment (Figure 3B). This is consistent with other published studies using
19 oncolytic viruses [20]. Triple immunofluorescence analysis of tumor sections revealed an
20 increase in activated CD8⁺ cytotoxic T cells (i.e. IFN γ ⁺ or PD-1⁺ CD3⁺CD8⁺ cells) in this
21 mouse model after HSV1716 treatment (Figure 3C). Furthermore, HSV1716 treatment led to
22 a reduction in the number of CD4⁺FOXP3⁺ T regulatory (Treg) cells (Figure 3D).

23

24 **HSV1716 reprograms TAMs to a more pro-inflammatory and perivascular phenotype**

25 NanoString nCounter™ gene profiling revealed an upregulation in the macrophage function
26 scores (Supplementary Fig. 3B). Despite this, we observed the average number of TAMs

1 within tumor samples (% of CD45⁺F4/80⁺ per 100,000 events of viable cells) was not
2 significantly altered following HSV1716 treatment (Figure 3B), but that there was a marked
3 change in their phenotype. First, HSV1716 treatment significantly decreased the prevalence
4 of “tumour promoting” perivascular macrophages (i.e. F4/80⁺ TAMs directly in contact with
5 CD31⁺ endothelial cells) in PyMT mammary tumors (Figure 4A). Second, HSV1716
6 treatment significantly increased the number of F4/80⁺ TAMs expressing pro-inflammatory,
7 M1-like markers, IL-12 and iNOS, relative to matched controls (no virus). Furthermore,
8 HSV1716 treatment significantly reduced ($P < 0.05$) the number of F4/80⁺ TAMs expressing
9 the M2-like marker ‘MRC1’ (Figure 4B). This reprogramming of TAMs has the potential to
10 change the balance in the TME, in that M2-like TAMs become M1-like, thereby promoting
11 the recruitment of adaptive immune cells and cytotoxic potential.

12

13 Our *in vitro* experiments also demonstrated that human MDMs infected with HSV1716
14 undergo a transformation to a more inflammatory phenotype, specifically a greater
15 expression of M1-like markers (CD80^{hi}, CD86^{hi}, PD-L1^{hi}) and lower expression of M2-like
16 markers (CD64^{lo}, CD163^{lo} and CD206/MRC1^{lo}) (Supplementary Fig. S4A) and increases in
17 the expression of pro-inflammatory vs. anti-inflammatory markers at the mRNA level
18 (Supplementary Fig. S4B). Infected macrophages also secreted pro-inflammatory cytokines
19 including IL-6, IL-12 and TNF α (Supplementary Fig. S4C) and increased levels of nitric oxide
20 (Supplementary Fig. S4D).

21

22 **Macrophages support HSV1716 replication and undergo immunogenic cell death**

23 The observation that HSV1716 treatment led to a co-localisation of F4/80⁺ TAMs and
24 HSV1716 in the TME (Figure 5A), prompted the question as to whether macrophages are
25 permissive to HSV1716 infection and, if so, what is the nature of this relationship? To
26 investigate this, MDMs derived from human buffy coats were infected with the HSV1716 for
27 2 hours, following which excess virus was washed off, cells incubated for a further 24 hours
28 and infection confirmed on the basis of GFP expression using the reporter virus

1 (HSV1716:GFP) (Figure 5B). Plaque assays determined viral titres within the supernatants
2 of these virally infected MDMs. An increase in viral titres at 24, 48 and 72 hours was seen
3 following infection of the HSV permissive Vero cell line (Figure 5C). Furthermore, expression
4 of genes required for early (ICP0), mid (ICP8) and late (gB) viral replication was quantified
5 using qPCR (Figure 5D). These studies confirmed that HSV1716 went through all stages of
6 viral replication within MDMs *in vitro* and suggest that MDMs infected with HSV1716
7 supported active viral replication.

8

9 As we saw a significant drop in macrophage numbers 24 hours after treatment *in vivo*
10 (Supplementary Fig. S5A), we next assessed the impact of HSV1716 on macrophage
11 viability and sought to identify the cause of this in human MDMs *in vitro*. First, we noted that
12 human MDMs infected with HSV1716 undergo enhanced levels of cell death compared to
13 non-infected cells *in vitro* (Supplementary Fig. 5B). To ascertain the mechanism of this, a
14 cell death array was performed (Supplementary Table 4). The mechanism of macrophage
15 cell death and signalling pathways were largely apoptotic and immunogenic, with an
16 increase in Fas ligand and HMGB1 expression, and a down regulation of HSP genes
17 (validated by qPCR) (Supplementary Fig. S5C). These data were supported by Western
18 blots showing an increased production of apoptotic proteins, FADD, FASL and caspase 3,
19 (Supplementary Fig. S5D) and ELISA assays showing an increased secretion of
20 immunogenic proteins, HMGB1 (Supplementary Fig. S5E) and extracellular ATP
21 (Supplementary Fig. S5F).

22

23 **Proliferating cell nuclear antigen (PCNA) mediates HSV1716 replication in TAMs**

24 Oncolytic virus replication is known to occur within dividing tumor cells and therefore we
25 were keen to determine why HSV1716 was replicating within macrophages (i.e. terminally
26 differentiated cells). Wild type HSV has been shown to initiate proliferation in non-
27 proliferative cells such as neurones by interacting with the cellular protein, PCNA [21],
28 although this has not previously been demonstrated in macrophages. Interestingly, we found

1 that HSV1716-infected PyMT-TS1 tumors contained significantly more PCNA⁺ TAMs
2 (Figure. 6A).

3

4 PCNA expression in HSV1716 infected and non-infected MDMs was measured *in vitro* at
5 both the gene and protein level. MDMs infected with HSV1716 exhibited significant relative
6 increases in PCNA mRNA (11-fold increase, $p=0.0137$) and protein expression ($p=0.0173$)
7 compared with untreated MDMs (Supplementary Fig. S6A). This increased expression was
8 more marked when MDMs were infected with HSV1716 in the presence of tumor-
9 conditioned medium (TCM) (Figure. 6B). Given the increase in PCNA following infection we
10 wanted to ascertain whether HSV1716 replication was possible in the absence of PCNA.
11 PCNA knockdown (PCNA^{KD}) was carried out using Accell siRNA (Supplementary Fig. S6B).
12 This had no effect on viral infectivity and the viability of macrophages compared to the non-
13 targeting control (Supplementary Fig. S6C and S6D). Indeed, in the absence of PCNA,
14 HSV1716 was unable to undergo viral replication within infected macrophages. This is
15 evidenced by the lack of cell death in MDA-MB-231 cells following incubation with
16 supernatants taken from infected macrophage cultures following PCNA^{KD} (Figure 6C) and a
17 reduction in viral replication genes (Figure 6D). We therefore speculate that the presence of
18 PCNA is likely the cause of viral replication and macrophage cell death after infection.

19

20 Given the interactions between HSV1716 and macrophages, we then investigated the role of
21 macrophages in the anti-tumor responses seen with this oncolytic virus in our *in vivo* model.
22 To explore this, circulating monocytes and macrophages were eliminated *in vivo* using
23 clodronate liposomes [22] (Figure 7A). Clodronate liposomes induce the apoptosis of
24 macrophages and others have shown that this to trigger anti-tumor activity by inducing
25 changes in the TME [23]. We administered a single dose of clodronate at 48 hours prior to
26 treatment with HSV1716 and noticed a modest reduction in macrophage number (control
27 (PBS) 69.4 +/- 11.4, clodronate alone 33.9 +/-11.6, $p=0.0001$). As expected, IV HSV1716
28 decreased tumor growth in comparison to PBS controls. However, this effect was lost when

1 monocytes/macrophages were depleted, in that there was an increase in primary tumor
2 growth (Figure 7B) and a development of lung metastases when data for HSV1716
3 treatment are compared in the presence (OV+CL) or absence (OV) of clodronate liposomes
4 for simplicity (Figure 7C). Of note, a greater number of lung metastases were seen in this
5 experiment compared to the data presented in Figure 1B. This is likely due to the endpoint in
6 this experiment being later (day 14) as opposed to day 9 in Figure 1B. T cell subsets in
7 these two groups were examined using immunofluorescence post-mortem. An increase in
8 the number of CD4⁺ T cells and a decrease in CD8⁺ T cells were seen in animals in which
9 macrophages had been eliminated (Figure 7D). These data suggest that TAMs are key to
10 the cytotoxicity of HSV1716 infection *in vivo* and may mediate this through their regulation of
11 T cell subsets in the TME. The interaction between macrophages and T cells was also
12 confirmed in a human mixed lymphocyte population whereby the introduction of HSV1716, in
13 the presence of MDMs, resulted in a shift to activated CD4⁺ and CD8⁺ T cells with an
14 increase in the expression of the co-stimulatory receptor 4-1BB, OX40 (TNF superfamily
15 members) and PD-1 (Supplementary Fig. S7 A&B). No T cell activation was noted in
16 cultures with uninfected macrophages.

17

18 **Discussion**

19 Previous studies have investigated the effect of OV on the survival of malignant cells and the
20 number and activation status of lymphocyte subsets in tumors [24-26]. Although the effect of
21 OVs on TAMs has not been fully ascertained, primary brain tumors of patients that received
22 intravenous oncolytic reovirus had an unexpected increase in TAMs, suggesting that the role
23 of TAMs in OV therapy should be investigated further [9]. Here we show that TAMs play an
24 important role in mediating the anti-tumor effects of HSV1716. The virus had pronounced
25 effects on the phenotype of these cells and their depletion within the TME reversed the
26 tumoricidal effect of the OV.

27 TAMs are abundant in most breast tumors [27] and high numbers correlate with reduced
28 patient survival [28-31]. This accords with various studies in mice showing that these cells

1 stimulate angiogenesis and metastasis in mammary tumors [32, 33]. Macrophages show
2 high plasticity and can move along a continuum between two polarised activation states;
3 'classically activated', anti-tumor, 'M1-like' TAMs, and 'alternatively activated', tumor-
4 promoting immunosuppressive, 'M2-like TAMs [34]. The latter have been shown to limit
5 tumor responses to various treatments. In our work, we show that although macrophage
6 numbers are stable, there is a marked reduction in the MRC1+ and perivascular
7 macrophages within our tumors after treatment with HSV1716.

8

9 In contrast, M1-like TAMs can stimulate cytotoxic T cells by presenting cancer cell antigens
10 to them [3]. This creates a pro-inflammatory tumor microenvironment through the release of
11 cytokines (IL-1, IL-2, IL-6, and IL-12), superoxide anions and nitrogen free radicals.
12 Generally, studies have shown TAMs to be associated with poor patient prognosis and may
13 help facilitate cancer growth [2, 35, 36]. In our study, it is unclear whether the TAM variation
14 is causally linked to the size of the tumours. However like others, we see the re-education of
15 TAMs from an M2-like phenotype to more M1-like is associated with improved survival [37,
16 38]. Additionally, current evidence suggests that depletion or modification of TAMs alone
17 may result in increased survival *in vivo* [39, 40].

18

19 The ability of an OV to reprogram macrophages from an immunosuppressive to an
20 immunostimulatory phenotype opens the potential for OV to be used in conjunction with
21 immunotherapies. Immune checkpoint inhibition involving the blockade of the PD1-PDL1
22 pathway is currently being promoted in many tumor types. This acts to release an inhibitory
23 break thus allowing T cells to perform their cytotoxic function. In breast cancer, checkpoint
24 inhibitor monotherapy has a mixed response. This may be due to a failure of activation and
25 migration of CD8⁺ cytotoxic T cells within the TME. Given their ability to present antigen and
26 regulate the anti-tumor functions of T cells, macrophage modification may be key to
27 enhancing this. Indeed, it has been shown that combining PD-1 inhibition (to take the 'brake'
28 off T cells) and CSF-1 receptor blockade (to deplete TAMs within the TME) increases T cell

1 activation and recruitment within MMTV-PyMT derived MET-1 tumors, thereby increasing the
2 efficacy of the immunotherapy [41].

3

4 However, our data show that macrophages may also play an important role in enhancing OV
5 cytotoxicity by supporting viral amplification. We have previously shown that macrophages
6 can be loaded with OV *ex vivo* and, upon injection into the circulation of tumor-bearing mice,
7 deliver it to tumors [16, 42]. In this, we observed an HSV1716 appeared to be amplified by
8 macrophages. Our current work confirms that macrophages not only have the ability to take
9 up HSV1716, enable viral replication and release more HSV1716 particles *in vitro*, but also
10 re-educate macrophages in the process. Therefore we presume, the lysis of cancer cells by
11 HSV1716 is mediated by direct effects on cancer cells, resulting in immunogenic cell death,
12 and indirect effects on T cells, via TAMs, in the TME.

13

14 The ability of HSV1716 to reduce the growth and spread of cancer in our mouse mammary
15 models demonstrates that this may be useful for the treatment of breast cancer and warrants
16 clinical evaluation. HSV1716 is reported to have a good safety profile in non breast cancer
17 early phase clinical trials [12, 13] and lends well to seamlessly moving towards translating
18 this research from the bench to the bedside of patients with breast cancer. Our findings
19 indicate that the efficacy of treatments such as checkpoint inhibitors, which require activated
20 T cells to be present in tumors, may be enhanced when used in conjunction with HSV1716.

21

22 Previous studies have demonstrated the ability of macrophages to support the replication of
23 highly infective viruses such as the RNA viruses, influenza [43] and simian
24 immunodeficiency virus [44]. We believe we are the first to describe that cancer-killing OV
25 replication occurs within macrophages and that this may enhance virotherapy. Herein, we
26 show that PCNA expression by macrophages supports the replication of HSV1716 in a
27 PCNA-dependent manner. PCNA is an essential component of the “replication and repair”
28 machinery of cells but also shown to be involved in the HSV replication cycle [45, 46]. It has

1 been proposed that Neurovirulence Factor ICP34.5 is needed to allow PCNA mediated viral
2 replication in non-dividing cells, with studies showing ICP34.5 deleted HSV strains are
3 avirulent in non-dividing central nervous system neuronal lines [21, 47]. In tumor cells, PCNA
4 is already “switched on” for cellular DNA replication and ICP34.5 is not required to initiate
5 viral replication [45]. Studies comparing the replication of wild type and ICP34.5 deleted
6 HSV1 in Vero (African Green Monkey kidney epithelial) cells demonstrated that viral
7 replication was inhibited when PCNA expression had been knocked down [46]. The
8 implications of this are that PCNA plays a role in HSV DNA replication and that this might be
9 independent of ICP34.5. In untreated breast cancer, high numbers of PCNA-positive TAMs
10 correlate with an immunosuppressive TME and with poor patient prognosis [48-50]. In our *in*
11 *vitro* work, exposure of macrophages to tumor-conditioned medium increased their
12 intracellular expression of PCNA suggesting that cancer cells may stimulate TAMs to
13 express a phenotype that supports viral replication. It remains to be seen whether patients
14 with high numbers of PCNA-expressing TAMs respond better to HSV1716 than those with
15 low numbers. If so, this could be a new way to stratify patients for such form of OV therapy.

16

17 **Acknowledgements**

18 Thank you to Prof Johanna Joyce (MSKCC, USA) and Dr Jessalyin Ubellacker (University of
19 Harvard, USA) for providing the TS1 and E0771 cell lines respectively. AK & MM would like
20 to thank Virttu Biologics and CRUK (grant reference: C25574/A24321) and Sheffield
21 Teaching Hospitals Charity (grant reference: 12053) and Team Verrico (grant reference:
22 MS/149394) for their support for various aspects of this work. This project has also received
23 funding from the European Union’s Horizon 2020 research and innovation programme under
24 the Marie Skłodowska-Curie grant agreement number 872860-PRISAR2. We are also
25 grateful to Virttu Biologics for providing the HSV1716 for this work.

26

27

28

1 References

- 2 1. Sharma P. and Allison J.P., *The future of immune checkpoint therapy*. Science, 3 2015. **348**(6230): p. 56-61.
- 4 2. Lewis C.E., Harney A.S., and Pollard J.W., *The Multifaceted Role of Perivascular* 5 *Macrophages in Tumors*. Cancer Cell, 2016. **30**(2): p. 365.
- 6 3. Williams C.B., Yeh E.S., and Soloff A.C., *Tumor-associated macrophages: unwitting* 7 *accomplices in breast cancer malignancy*. NPJ Breast Cancer, 2016. **2**.
- 8 4. Kioi M., Vogel H., Schultz G., Hoffman R.M., Harsh G.R., and Brown J.M., *Inhibition* 9 *of vasculogenesis, but not angiogenesis, prevents the recurrence of glioblastoma* 10 *after irradiation in mice*. J Clin Invest, 2010. **120**(3): p. 694-705.
- 11 5. Hughes R., Qian B.Z., Rowan C., Muthana M., Keklikoglou I., Olson O.C., et al., 12 *Perivascular M2 Macrophages Stimulate Tumor Relapse after Chemotherapy*. 13 *Cancer Res*, 2015. **75**(17): p. 3479-91.
- 14 6. Dijkgraaf E.M., Heusinkveld M., Tummers B., Vogelpoel L.T., Goedemans R., Jha V., 15 *et al.*, *Chemotherapy alters monocyte differentiation to favor generation of cancer-* 16 *supporting M2 macrophages in the tumor microenvironment*. *Cancer Res*, 2013. 17 **73**(8): p. 2480-92.
- 18 7. Ribas A., Dummer R., Puzanov I., VanderWalde A., Andtbacka R.H.I., Michielin O., 19 *et al.*, *Oncolytic Virotherapy Promotes Intratumoral T Cell Infiltration and Improves* 20 *Anti-PD-1 Immunotherapy*. *Cell*, 2017. **170**(6): p. 1109-1119 e10.
- 21 8. Bourgeois-Daigneault M.C., Roy D.G., Aitken A.S., El Sayes N., Martin N.T., Varette 22 O., et al., *Neoadjuvant oncolytic virotherapy before surgery sensitizes triple-negative* 23 *breast cancer to immune checkpoint therapy*. *Sci Transl Med*, 2018. **10**(422).
- 24 9. Samson A., Scott K.J., Taggart D., West E.J., Wilson E., Nuovo G.J., et al., 25 *Intravenous delivery of oncolytic reovirus to brain tumor patients immunologically* 26 *primes for subsequent checkpoint blockade*. *Sci Transl Med*, 2018. **10**(422).
- 27 10. Andtbacka R.H., Kaufman H.L., Collichio F., Amatruda T., Senzer N., Chesney J., et 28 *al.*, *Talimogene Laherparepvec Improves Durable Response Rate in Patients With* 29 *Advanced Melanoma*. *J Clin Oncol*, 2015. **33**(25): p. 2780-8.
- 30 11. Benencia F., Courreges M.C., Conejo-Garcia J.R., Mohamed-Hadley A., Zhang L., 31 Buckanovich R.J., et al., *HSV oncolytic therapy upregulates interferon-inducible* 32 *chemokines and recruits immune effector cells in ovarian cancer*. *Mol Ther*, 2005. 33 **12**(5): p. 789-802.
- 34 12. Streby K.A., Geller J.I., Currier M.A., Warren P.S., Racadio J.M., Towbin A.J., et al., 35 *Intratumoral Injection of HSV1716, an Oncolytic Herpes Virus, Is Safe and Shows* 36 *Evidence of Immune Response and Viral Replication in Young Cancer Patients*. *Clin* 37 *Cancer Res*, 2017. **23**(14): p. 3566-3574.
- 38 13. Mace A.T., Ganly I., Soutar D.S., and Brown S.M., *Potential for efficacy of the* 39 *oncolytic Herpes simplex virus 1716 in patients with oral squamous cell carcinoma*. 40 *Head Neck*, 2008. **30**(8): p. 1045-51.
- 41 14. Shree T., Olson O.C., Elie B.T., Kester J.C., Garfall A.L., Simpson K., et al., 42 *Macrophages and cathepsin proteases blunt chemotherapeutic response in breast* 43 *cancer*. *Genes Dev*, 2011. **25**(23): p. 2465-79.
- 44 15. Ranjan A., Gupta P., and Srivastava S.K., *Penfluridol: An Antipsychotic Agent* 45 *Suppresses Metastatic Tumor Growth in Triple-Negative Breast Cancer by Inhibiting* 46 *Integrin Signaling Axis*. *Cancer Res*, 2016. **76**(4): p. 877-90.
- 47 16. Muthana M., Giannoudis A., Scott S.D., Fang H.Y., Coffelt S.B., Morrow F.J., et al., 48 *Use of macrophages to target therapeutic adenovirus to human prostate tumors*. 49 *Cancer Res*, 2011. **71**(5): p. 1805-15.
- 50 17. Huber S., Hoffmann R., Muskens F., and Voehringer D., *Alternatively activated* 51 *macrophages inhibit T-cell proliferation by Stat6-dependent expression of PD-L2*. 52 *Blood*, 2010. **116**(17): p. 3311-20.

- 1 18. Muthana M., Hawtree S., Wilshaw A., Linehan E., Roberts H., Khetan S., *et al.*,
2 *C5orf30 is a negative regulator of tissue damage in rheumatoid arthritis*. Proc Natl
3 Acad Sci U S A, 2015. **112**(37): p. 11618-23.
- 4 19. Baer A. and Kehn-Hall K., *Viral concentration determination through plaque assays:
5 using traditional and novel overlay systems*. J Vis Exp, 2014(93): p. e52065.
- 6 20. Thomas D.L. and Fraser N.W., *HSV-1 therapy of primary tumors reduces the number
7 of metastases in an immune-competent model of metastatic breast cancer*. Mol Ther,
8 2003. **8**(4): p. 543-51.
- 9 21. Kennedy P.G., Gairns J., and MacLean A.R., *Replication of the herpes simplex virus
10 type 1 RL1 mutant 1716 in primary neuronal cell cultures--possible relevance to use
11 as a viral vector*. J Neurol Sci, 2000. **179**(S 1-2): p. 108-14.
- 12 22. van Rooijen N. and Sanders A., *Elimination, blocking, and activation of
13 macrophages: three of a kind?* J Leukoc Biol, 1997. **62**(6): p. 702-9.
- 14 23. Denton N.L., Chen C.Y., Hutzen B., Currier M.A., Scott T., Nartker B., *et al.*,
15 *Myelolytic Treatments Enhance Oncolytic Herpes Virotherapy in Models of Ewing
16 Sarcoma by Modulating the Immune Microenvironment*. Mol Ther Oncolytics, 2018.
17 **11**: p. 62-74.
- 18 24. Tan D.Q., Zhang L., Ohba K., Ye M., Ichiyama K., and Yamamoto N., *Macrophage
19 response to oncolytic paramyxoviruses potentiates virus-mediated tumor cell killing*.
20 Eur J Immunol, 2016. **46**(4): p. 919-28.
- 21 25. Denton N.L., Chen C.Y., Scott T.R., and Cripe T.P., *Tumor-Associated Macrophages
22 in Oncolytic Virotherapy: Friend or Foe?* Biomedicines, 2016. **4**(3).
- 23 26. Denton N.L.C., Hutzen B., Leddon J., Wang P.Y., Scott T., Currier M., Eubank T., Cripe
24 T.P., *Tumor Associated Macrophages Mitigate Oncolytic Herpes Simplex Virus
25 Efficacy in Part Through TGF- β Signaling*. Molecular Therapy, 2016. **Volume 24,**
26 **Supplement 1**: p. pS206–S207.
- 27 27. Kelly C.A., Ward C., Stenton S.C., Hendrick D.J., and Walters E.H., *Assessment of
28 pulmonary macrophage and neutrophil function in sequential bronchoalveolar lavage
29 aspirates in sarcoidosis*. Thorax, 1988. **43**(10): p. 787-91.
- 30 28. Zhao X., Qu J., Sun Y., Wang J., Liu X., Wang F., *et al.*, *Prognostic significance of
31 tumor-associated macrophages in breast cancer: a meta-analysis of the literature*.
32 Oncotarget, 2017. **8**(18): p. 30576-30586.
- 33 29. DeNardo D.G., Brennan D.J., Rexhepaj E., Ruffell B., Shiao S.L., Madden S.F., *et
34 al.*, *Leukocyte complexity predicts breast cancer survival and functionally regulates
35 response to chemotherapy*. Cancer Discov, 2011. **1**(1): p. 54-67.
- 36 30. Shabo I., Stal O., Olsson H., Dore S., and Svanvik J., *Breast cancer expression of
37 CD163, a macrophage scavenger receptor, is related to early distant recurrence and
38 reduced patient survival*. Int J Cancer, 2008. **123**(4): p. 780-6.
- 39 31. Kurahara H., Shinchi H., Mataka Y., Maemura K., Noma H., Kubo F., *et al.*,
40 *Significance of M2-polarized tumor-associated macrophage in pancreatic cancer*. J
41 Surg Res, 2011. **167**(2): p. e211-9.
- 42 32. Lin H., Chen C., and Chen B.D., *Resistance of bone marrow-derived macrophages to
43 apoptosis is associated with the expression of X-linked inhibitor of apoptosis protein
44 in primary cultures of bone marrow cells*. Biochem J, 2001. **353**(Pt 2): p. 299-306.
- 45 33. Lin E.Y., Li J.F., Gnatovskiy L., Deng Y., Zhu L., Grzesik D.A., *et al.*, *Macrophages
46 regulate the angiogenic switch in a mouse model of breast cancer*. Cancer Res,
47 2006. **66**(23): p. 11238-46.
- 48 34. Yang M., McKay D., Pollard J.W., and Lewis C.E., *Diverse Functions of
49 Macrophages in Different Tumor Microenvironments*. Cancer Res, 2018. **78**(19): p.
50 5492-5503.
- 51 35. Jakeman P.G., Hills T.E., Fisher K.D., and Seymour L.W., *Macrophages and their
52 interactions with oncolytic viruses*. Curr Opin Pharmacol, 2015. **24**: p. 23-9.
- 53 36. Murdoch C., Muthana M., Coffelt S.B., and Lewis C.E., *The role of myeloid cells in
54 the promotion of tumour angiogenesis*. Nat Rev Cancer, 2008. **8**(8): p. 618-31.

- 1 37. Tariq M., Zhang J., Liang G., Ding L., He Q., and Yang B., *Macrophage Polarization: Anti-Cancer Strategies to Target Tumor-Associated Macrophage in Breast Cancer*. J Cell Biochem, 2017. **118**(9): p. 2484-2501.
- 2
3
4 38. Georgoudaki A.M., Prokopec K.E., Boura V.F., Hellqvist E., Sohn S., Ostling J., et al., *Reprogramming Tumor-Associated Macrophages by Antibody Targeting Inhibits Cancer Progression and Metastasis*. Cell Rep, 2016. **15**(9): p. 2000-11.
- 5
6
7 39. Fritz J.M., Tennis M.A., Orlicky D.J., Lin H., Ju C., Redente E.F., et al., *Depletion of tumor-associated macrophages slows the growth of chemically induced mouse lung adenocarcinomas*. Front Immunol, 2014. **5**: p. 587.
- 8
9
10 40. Poh A.R. and Ernst M., *Targeting Macrophages in Cancer: From Bench to Bedside*. Front Oncol, 2018. **8**: p. 49.
- 11
12 41. Peranzoni E., Lemoine J., Vimeux L., Feuillet V., Barrin S., Kantari-Mimoun C., et al., *Macrophages impede CD8 T cells from reaching tumor cells and limit the efficacy of anti-PD-1 treatment*. Proc Natl Acad Sci U S A, 2018. **115**(17): p. E4041-E4050.
- 13
14
15 42. Muthana M., Rodrigues S., Chen Y.Y., Welford A., Hughes R., Tazzyman S., et al., *Macrophage delivery of an oncolytic virus abolishes tumor regrowth and metastasis after chemotherapy or irradiation*. Cancer Res, 2013. **73**(2): p. 490-5.
- 16
17
18 43. Cline T.D., Beck D., and Bianchini E., *Influenza virus replication in macrophages: balancing protection and pathogenesis*. J Gen Virol, 2017. **98**(10): p. 2401-2412.
- 19
20 44. Williams K., Schwartz A., Corey S., Orandle M., Kennedy W., Thompson B., et al., *Proliferating cellular nuclear antigen expression as a marker of perivascular macrophages in simian immunodeficiency virus encephalitis*. Am J Pathol, 2002. **161**(2): p. 575-85.
- 21
22
23
24 45. Harland J., Dunn P., Cameron E., Conner J., and Brown S.M., *The herpes simplex virus (HSV) protein ICP34.5 is a virion component that forms a DNA-binding complex with proliferating cell nuclear antigen and HSV replication proteins*. J Neurovirol, 2003. **9**(4): p. 477-88.
- 25
26
27
28 46. Sanders I., Boyer M., and Fraser N.W., *Early nucleosome deposition on, and replication of, HSV DNA requires cell factor PCNA*. J Neurovirol, 2015. **21**(4): p. 358-69.
- 29
30
31 47. Ward S.L., Scheuner D., Poppers J., Kaufman R.J., Mohr I., and Leib D.A., *In vivo replication of an ICP34.5 second-site suppressor mutant following corneal infection correlates with in vitro regulation of eIF2 alpha phosphorylation*. J Virol, 2003. **77**(8): p. 4626-34.
- 32
33
34
35 48. Campbell M.J., Tonlaar N.Y., Garwood E.R., Huo D., Moore D.H., Khramtsov A.I., et al., *Proliferating macrophages associated with high grade, hormone receptor negative breast cancer and poor clinical outcome*. Breast Cancer Res Treat, 2011. **128**(3): p. 703-711.
- 36
37
38
39 49. Campbell M.J., Wolf D., Mukhtar R.A., Tandon V., Yau C., Au A., et al., *The prognostic implications of macrophages expressing proliferating cell nuclear antigen in breast cancer depend on immune context*. PLoS One, 2013. **8**(10): p. e79114.
- 40
41
42 50. Mukhtar R.A., Moore A.P., Nseyo O., Baehner F.L., Au A., Moore D.H., et al., *Elevated PCNA+ tumor-associated macrophages in breast cancer are associated with early recurrence and non-Caucasian ethnicity*. Breast Cancer Res Treat, 2011. **130**(2): p. 635-44.
- 43
44
45
46
47
48
49
50
51

1 **Tables – none**

2

3 **Figures legends:**

4 **Figure 1: HSV1716 treatment inhibits primary mammary tumor growth and metastatic**

5 **spread.** PyMT-TS1, EO771 and 4T1 cells were implanted into the 4th mammary fat pad of

6 immuno-competent syngeneic female mice. When tumors reached ~150mm³, mice received

7 intravenous HSV1716 (dose 1x10⁶ PFU) or PBS. Tumor volume was assessed by caliper

8 measurements *in vivo* and pulmonary metastases were measured postmortem by H&E

9 staining. HSV1716 (grey line) significantly reduced (A) mammary tumor growth and (B)

10 subsequent development of lung metastases in all three models. Data shown are mean ±

11 SEM, n= 10 mice/treatment group and statistical significance analyzed using multiple t tests

12 where * = $P < 0.05$, ** = $P < 0.01$, *** = $P < 0.001$, **** = $P < 0.0001$ compared to control

13 (untreated cells).

14

15 **Figure 2: HSV1716 treatment prevents tumor spread in a model of metastatic seeding.**

16 Luciferase labeled 4T1 cells were injected into the left ventricles of female BALB/c mice. At

17 day 5, mice were treated with PBS, HSV1716 (1 X10⁷ PFU, single dose) or HSV1716 (1x10⁷

18 on days 5,7,9). (A) Schematic representation of the treatment schedule is shown. (B)

19 Representative images of metastatic burden in different treatment groups at day 20. Tumor

20 burden was inhibited in the OV treated group with no disease observed in the 3-dose group

21 at the end of experiment. (C) Overall survival was also increased in all mice that received

22 virus. There is a statistically significant reduction in the survival between the control

23 (phosphate-buffered saline, PBS, treated) and the group that received 3 doses of HSV1716

24 ($p = 0.0002$, CI 15.49-35.18) and between the OVx1 and OVx3 group ($p = 0.01$, CI 5.401 to

25 31.93). (D) Burden of metastases was calculated as the percentage of the organ with

26 metastatic involvement; this was calculated as an average between 4 slides in 2-4 different

27 sections of organ, over 100µm apart. Data shown are mean ± SEM, n = 6 animals. Statistical

28 significance was assessed by one-way ANOVA where * $P < 0.05$.

1 **Figure 3. HSV1716 treatment induces inflammation within the tumour**
2 **microenvironment (TME).** PyMT tumors were grown in syngeneic female FVB mice and
3 randomized into 2 treatment arms, control (PBS) and intravenous HSV1716 treatment (n=5-
4 10 per arm). (A) RNA was isolated from tumors and analysed using the NanoString
5 nCounter™ murine Pan-Cancer Immune Profiling Panel. Volcano plots show genes that
6 were up regulated or downregulated following IV HSV1716 treatment compared to tumors in
7 PBS-treated mice (n=3). The data were processed and analysed using nSolver™ Analysis
8 Software, using the Advanced Analysis module. (B) Flow cytometric data from these
9 enzymatically digested tumor specimens are shown from n=10 mice per group. Only viable
10 cells (UV-) were used in this analysis. Each immune cell population was gated upon based
11 on CD45 expression and the respective immune cell marker. This shows changes in the
12 percentage of infiltrating immune cells (myeloid cells (F480⁺), monocytes (Ly6C⁺),
13 neutrophils (Ly6G⁺), T cells (CD3⁺CD4⁺,CD8⁺)) within the TME. (C) Immunofluorescent
14 staining of respective tumors (5 fields per view per slide) confirmed that these T cells
15 become activated in response to HSV1716 treatment, as illustrated by increased expression
16 of IFN γ and PD1 and (D) a decrease in the prevalence of CD4⁺FOXP3⁺ immunoregulatory T
17 (Treg) cells. Data shown are mean \pm SEM, analysed by Student t tests where p<0.05.

18

19 **Figure 4. HSV1716 treatment reprograms TAMs to become less perivascular and more**
20 **pro-inflammatory.** (A) Sections of primary tumors, derived from the PyMT-TS1 model,
21 treated with intravenous HSV1716 (OV) or PBS show a significant decrease in the number
22 of perivascular (CD31⁺) macrophages after HSV1716 treatment (n=10 animals). These were
23 quantified by only counting the F4/80+ cells in direct contact with CD31+ cells. (B) HSV1716
24 treatment also causes a shift in macrophage phenotype with a down regulation in
25 F4/80⁺MRC1⁺ cells and a significant increase in presence of F4/80⁺IL-12⁺ and F4/80⁺iNOS⁺
26 cells. Images were taken using the Nikon A1 confocal microscope and scored using FIJI
27 image J software. Co-localization between F4/80 and MRC1, IL-12 or iNOS was determined
28 and quantified using the Cell Counter tool from ImageJ (Fiji) [National Institutes of Health

1 (NIH), Bethesda, MD, USA] and 5 randomly selected fields of view were imaged per tumor.
2 Data shown are mean \pm SEM, analysed by student t tests where $p < 0.05$.

3

4 **Figure 5. Monocyte-derived macrophages (MDMs) are permissive to HSV1716**

5 **infection and replication.** (A) Representative sections from primary PyMT TS1 tumors in

6 control (PBS) and HSV1716-treated mice showed co-localisation of F4/80⁺ macrophages
7 (green) and HSV1716 (white). This was quantified in $n=10$ animals, 5 fields per view. (B)

8 MDMs were infected with HSV1716 expressing GFP at MOI 5. *In vitro* infection was
9 assessed by flow cytometry (left image) and fluorescence (right image). (C) Supernatants

10 taken from these cultures were assessed by the plaque-forming assay on Vero cells and an
11 increase in viral titres over time suggested active viral replication within these macrophages.

12 (D) qPCR analysis of MDMs at 24 h post infection resulted in the mRNA expression of the
13 viral early-ICP0 (Left), mid-ICP8 (centre) and late-gB (right) replication genes. Data shown

14 are mean \pm SEM, analysed by student t test where $p < 0.05$, $n=5$ independent experiments.
15

16 **Figure 6. PCNA mediates HSV1716 replication in monocyte-derived macrophages**

17 **(MDMs).** Female FVB tumor-bearing mice (PyMT-TS1) received a single dose of
18 intravenous HSV1716 at 10^6 PFU (OV) or PBS (control). (A) PCNA expression by TAMs

19 (arrowed) is significantly upregulated in response to HSV1716 at day 9 post treatment ($n=5$
20 mice per group). (B) *In vitro* studies confirmed that PCNA expression at both the RNA and

21 protein level by MDMs significantly increases after infection. (C) Accell siRNA was used to
22 knock down PCNA (PCNA^{KD}) within MDMs. The human breast cancer cell line MDA-MB-231

23 was treated with supernatants from MDMs infected with HSV1716 (with or without PCNA^{KD})
24 at different MOIs. At 72 hours we see inhibition of viral induced cell death in cultures where

25 PCNA is knocked down. (D) PCNA knockdown also suppressed replication of virus infected
26 cells (MOI 5), as shown by qPCR of MDMs at 72 hours post infection with suppression of

27 early-ICP0 (Left), mid-ICP8 (centre) and late-gB (right) viral replication genes. Key: OV =

1 oncolytic virus and PCNA^{KD}+OV=PCNA knockdown and OV. Data shown are mean ± SEM
2 and analyzed using a one-way ANOVA where p<0.05, n=5 experiment

3

4 **Figure 7: HSV1716 cytotoxicity is dependent on macrophages and transforms**
5 **immunogenically ‘cold’ tumors to ‘hot’ tumors.** Orthotopically implanted PyMT-TS1
6 tumors were grown immunocompetent syngeneic female FVB mice. Macrophages were
7 eliminated by intravenous administration of clodronate liposomes 48 hours before
8 administration of HSV1716 (n=5 animals, 1 section, 5 fields per view per section). (A)
9 Clodronate liposomes decrease TAMs within the TME (brighter cells = F480⁺ cells). This
10 depletion of TAMs attenuated the influence of HSV1716 treatment on the growth of primary
11 tumors (B) and development of pulmonary metastases (C) *in vivo*. (D) An increase in helper
12 CD4⁺ T cells and a reduction in cytotoxic CD8⁺ cells was observed after HSV1716 treatment
13 (brighter cells). Data shown are mean ± SEM, one-way ANOVA where p<0.05, n=5
14 experiments.

15

16

17

18

19

20

21

22

23

24

25

26

27

28

1 **Figures:**

Figure 1

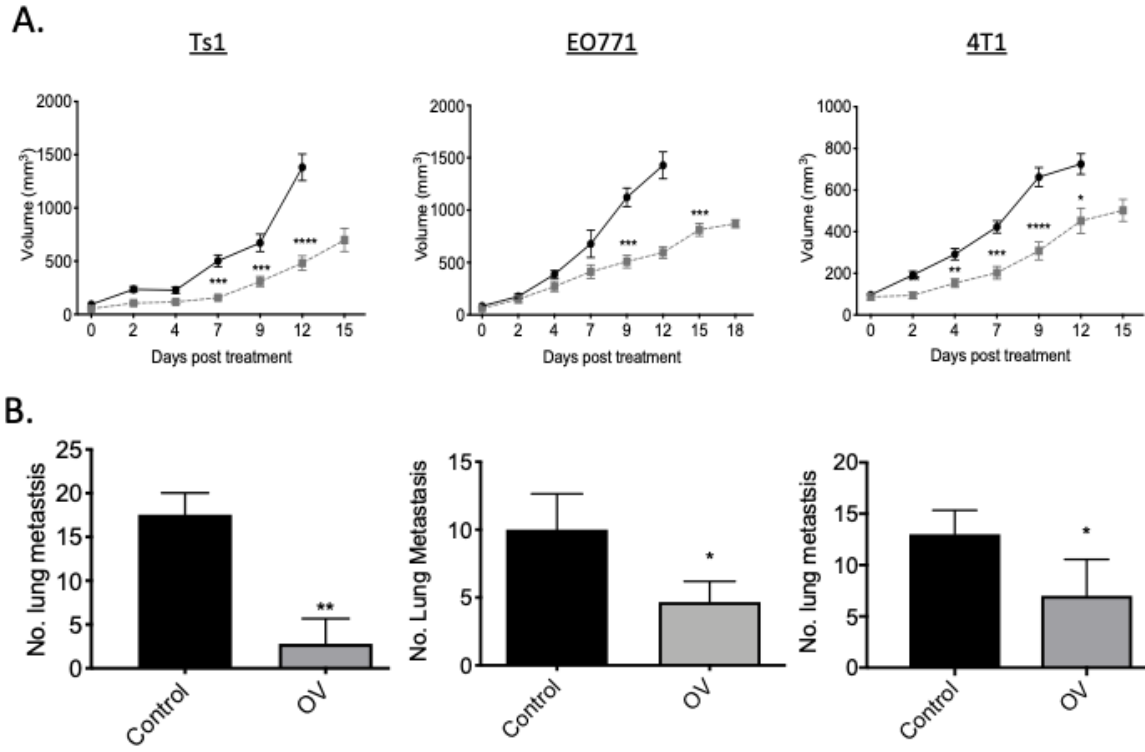


Figure 2

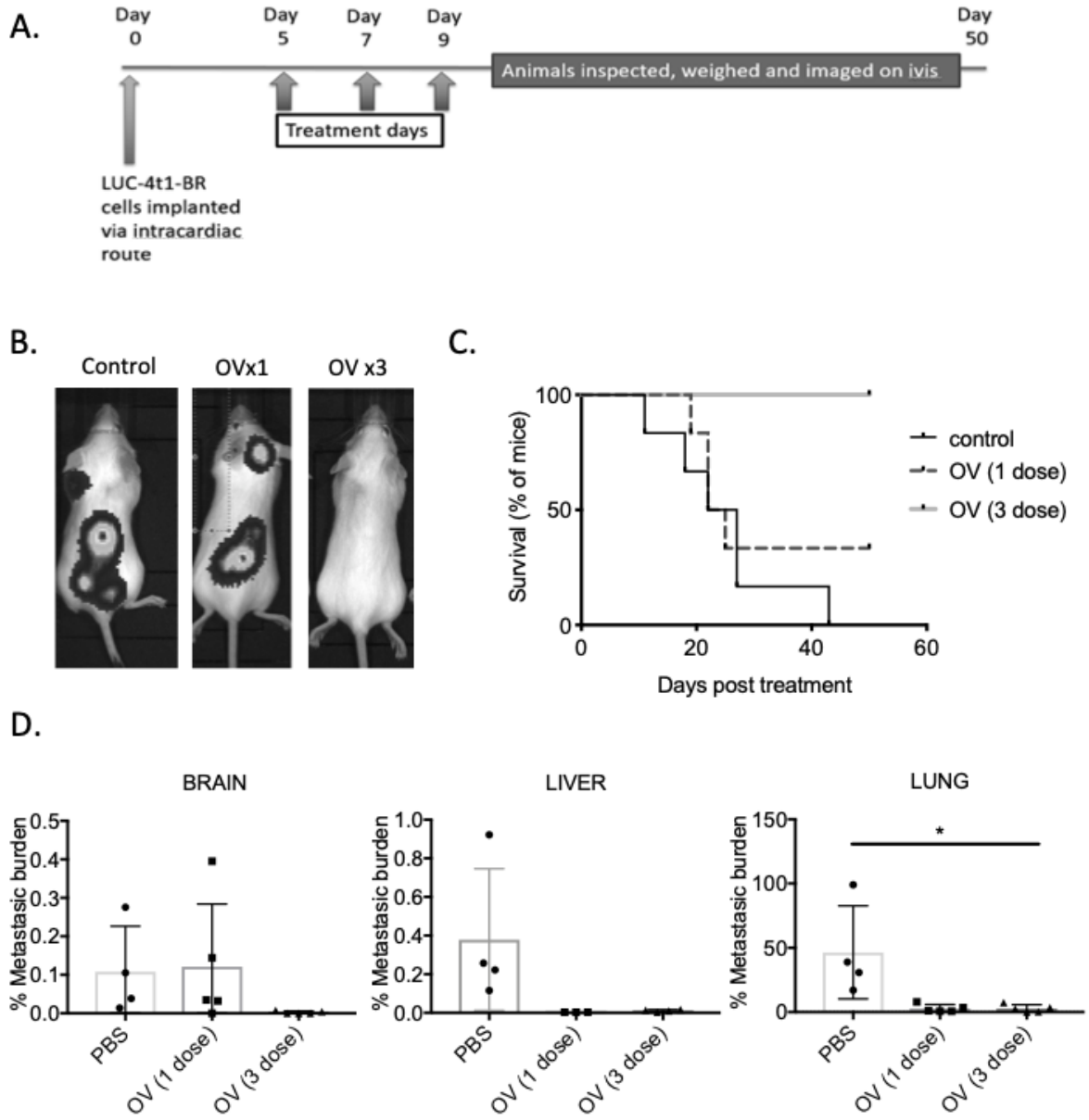


Figure 3

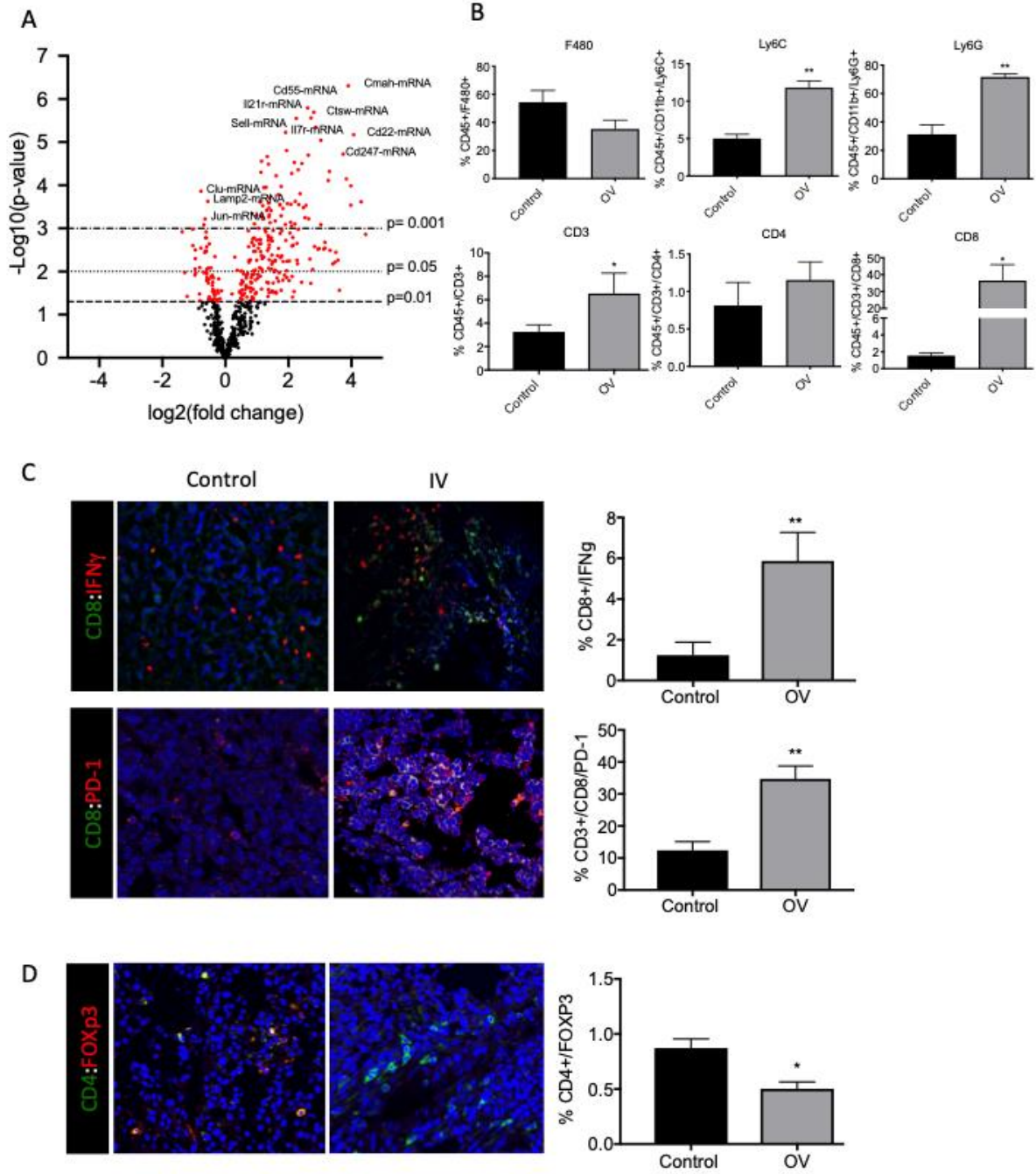


Figure 4

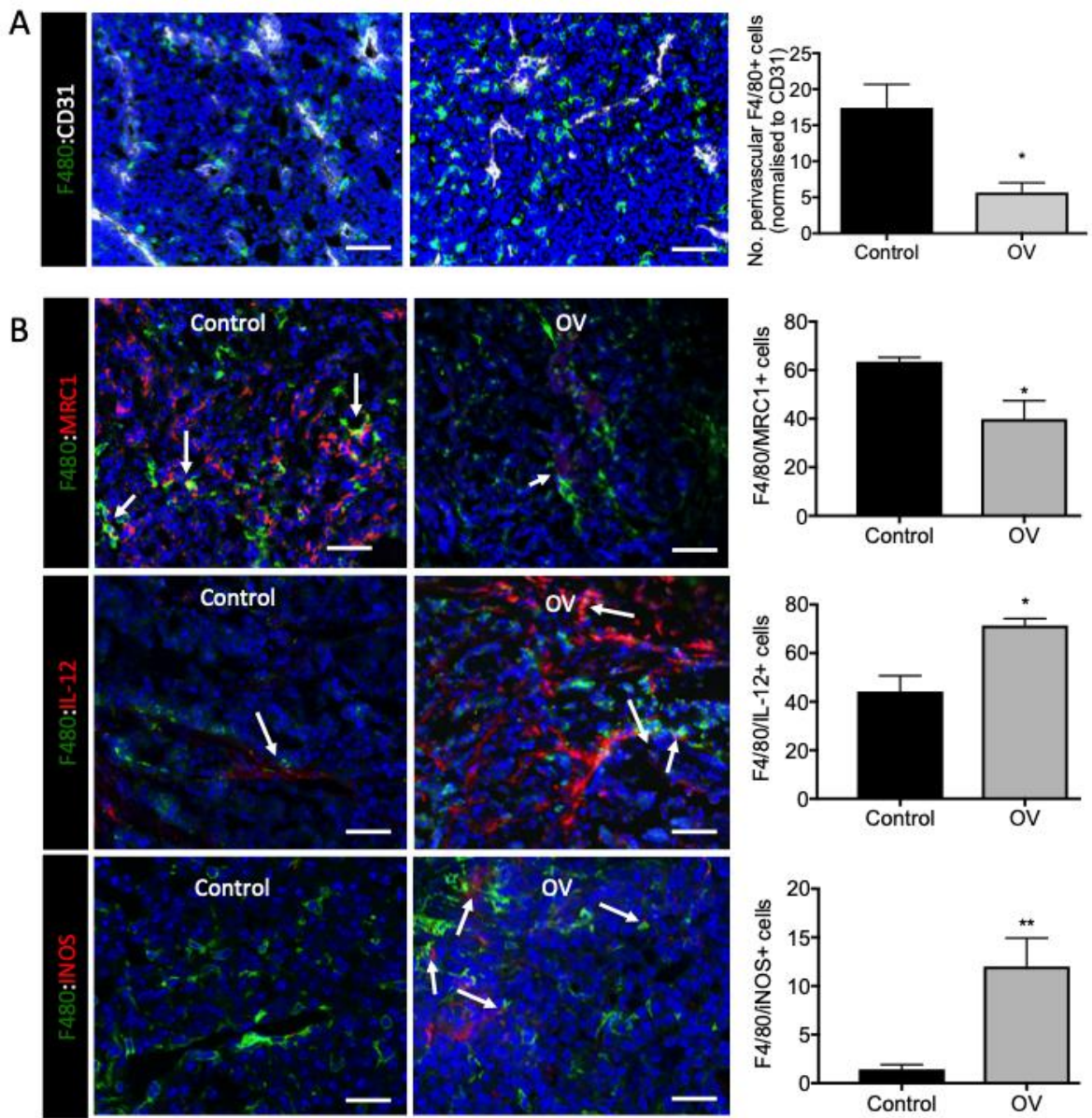


Figure 5

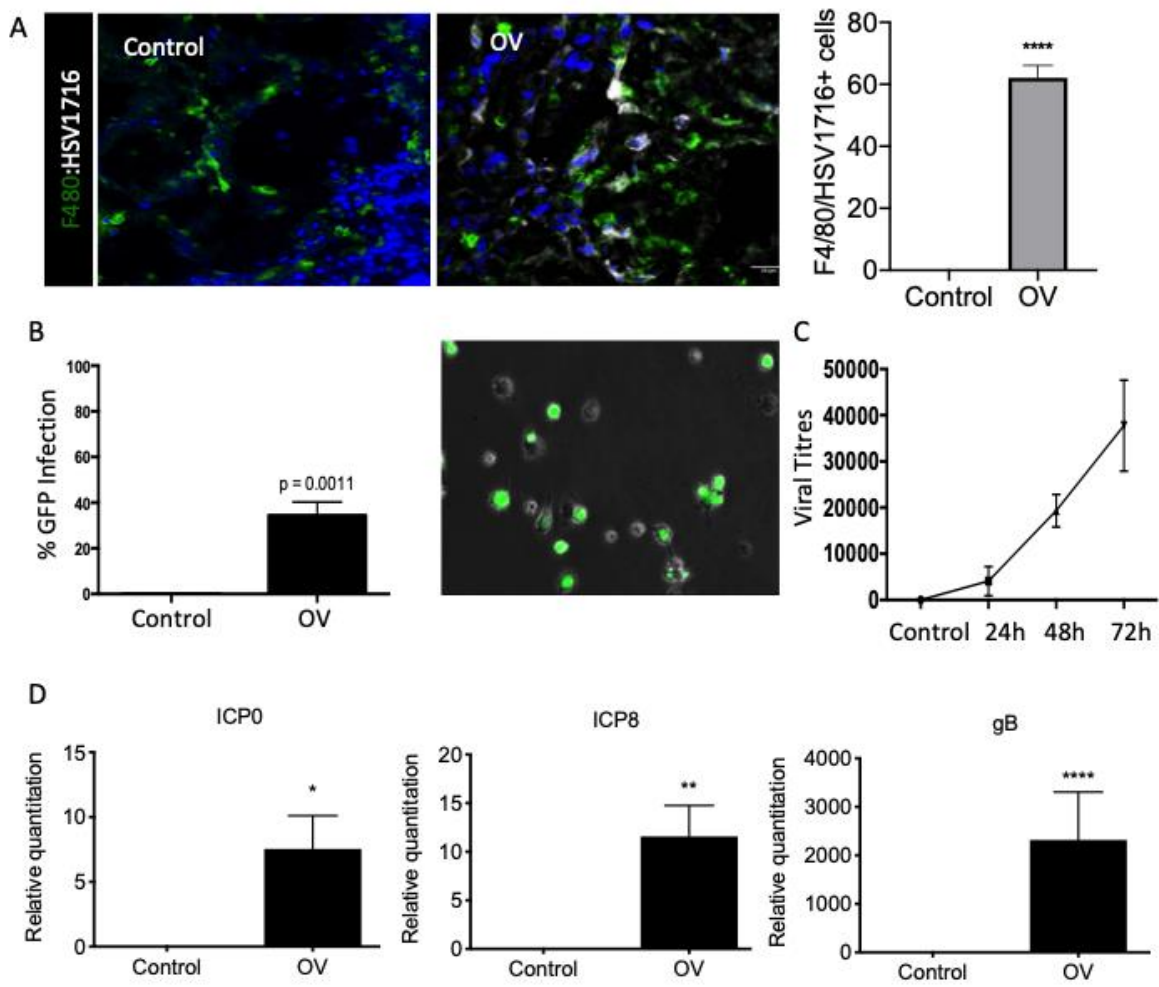


Figure 6

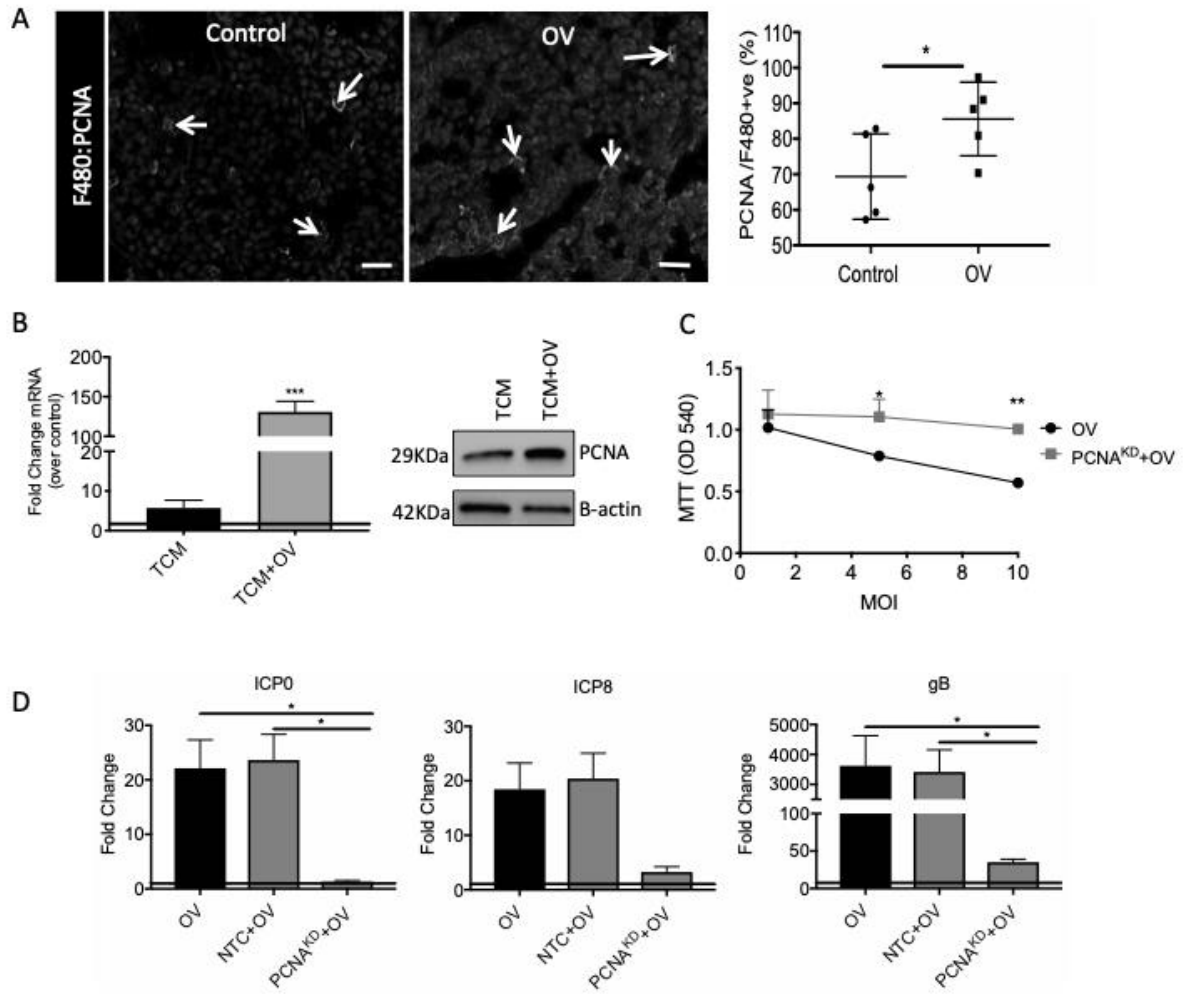
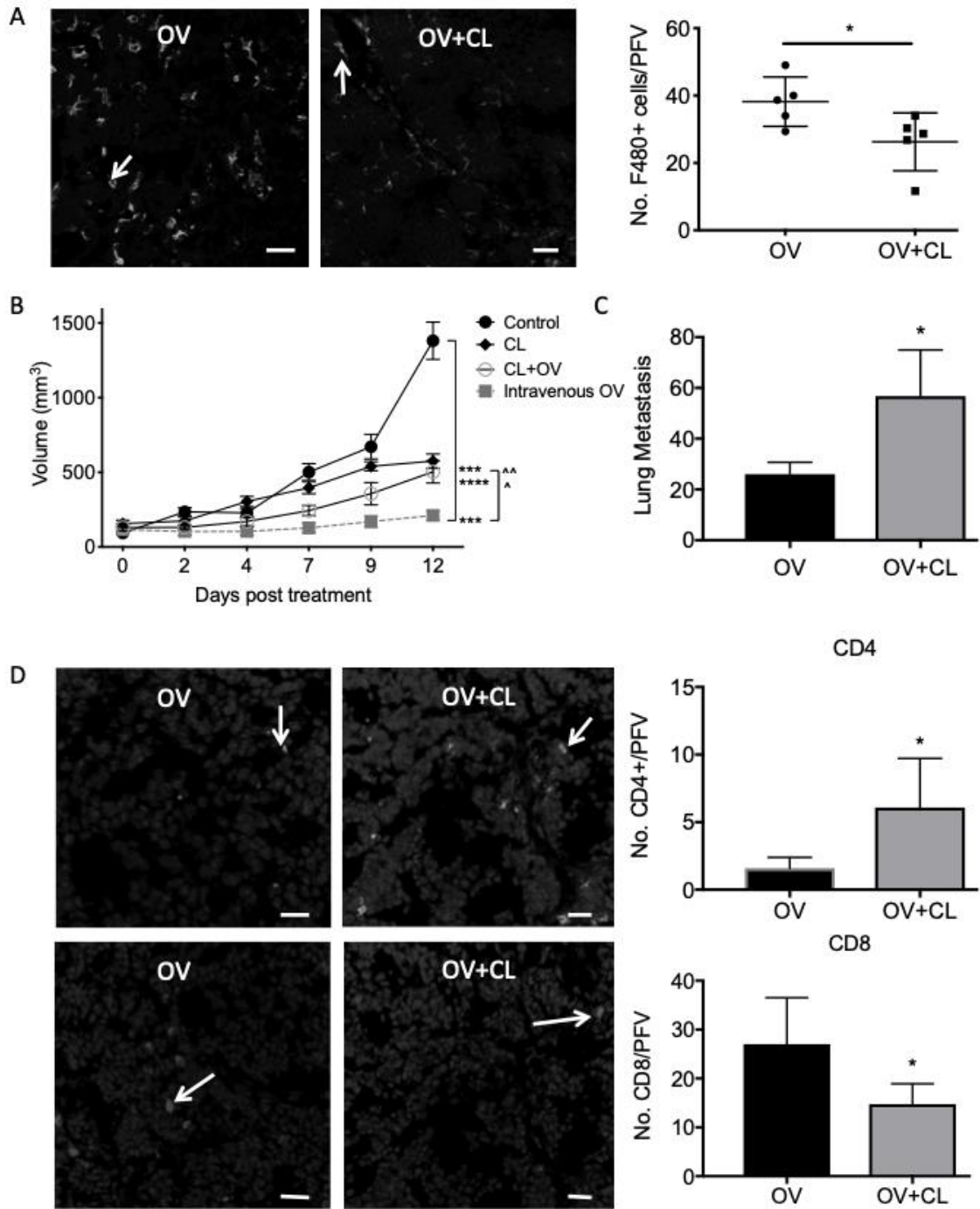


Figure 7



1

2

3